

VIBRATIONAL BEHAVIOR OF ADAPTIVE AIRCRAFT WING STRUCTURES
 MODELLED AS COMPOSITE THIN-WALLED BEAMS

O. Song, L. Librescu
 Engineering Science and Mechanics Department
 Virginia Polytechnic Institute and State University
 Blacksburg, VA

C. A. Rogers
 Center for Intelligent Material Systems and Structures
 Virginia Polytechnic Institute and State University
 Blacksburg, VA

515-24
 51384
 P-21

SUMMARY

The vibrational behavior of cantilevered aircraft wings modeled as thin-walled beams and incorporating piezoelectric effects is investigated. Based on the converse piezoelectric effect, the system of piezoelectric actuators conveniently located on the wing yield the control of its associated vertical and lateral bending eigenfrequencies. The possibility revealed by this study enabling one to increase adaptively the eigenfrequencies of thin-walled cantilevered beams could play a significant role in the control of the dynamic response and flutter of wing and rotor blade structures.

INTRODUCTION

The successful development of smart material systems technology [R1] is likely to generate new avenues and concepts toward the design of the next generation of aeronautical and aerospace vehicles. In spite of the complexity and severity of environmental conditions to which these vehicles are likely to be exposed, they must be designed as to be capable to operate safely within their flight envelope, at higher angles of attack, at superior speeds, and without weight penalties. The implementation of smart material systems could play an important role in the design of future advanced space vehicles.

As is well known, in the determination of both the dynamic response to time-dependent excitations and of resonant conditions as well as in the flutter analyses, the natural frequencies are an important physical parameter that intervenes in an explicit way [R2]. For this reason, one of the features of adaptive structural technology applied to aeronautical structures is the ability to conveniently control the eigenfrequencies of the system. In an effort to contribute to this problem, the free vibration analysis of adaptive aircraft wing structures incorporating induced strain actuation [R3,4] will be considered in this paper. The wing structure modelled as a thin-walled beam is assumed to be composed of an induced strain actuator, e.g. a piezoelectric layer superposed on the master structure.

The global constitutive equations associated with a piezoelectric material layer (the induced strain actuator), polarized in the thickness direction and exhibiting transversely isotropic properties, superposed on the thin-walled beam structure also made of a transversely-isotropic material, are derived. These equations, used in conjunction with a generalized Hamilton's variational principle [R5,6], yield the equations governing the motion of cantilevered adaptive

wing structure modelled as a thin-walled beam. Coupling the basic properties of piezoelectric materials (i.e., their actuating capabilities) with a control law, it will be shown that the natural frequencies can be controlled in a known and predictable manner.

BASIC ASSUMPTIONS

The thin-walled beam model used in the present paper is based on the following kinematic statements [R8-12]:

- 1) The original shape of the cross-sections of the beam is preserved.
- 2) The transverse shear flexibility exhibited by the advanced composite material structures is incorporated.
- 3) The non-uniform torsional model is considered. In this respect, the rate of twist assumed to vary along the beam axis constitutes a measure of the warping restraint effect. The primary warping displacement, throughout the cross-section of a beam, is assumed to have a similar distribution as the one associated with the St. Venant (uniform) torsion theory.
- 4) Incorporation of the secondary warping [R9] whose effect for composite material structures could be comparable to the primary warping.
- 5) In addition to these statements of kinematic nature, another one, of a static nature is adopted [R10]. According to this statement, the hoop stress resultant $N_{\theta\theta}$ is considered negligibly small with respect to the remaining ones.

Based on the above assumptions, the displacement field can be expressed as [see R7-9]:

$$u(x,y,z) = u_0(z) - y\Theta(z), \quad (1)$$

$$v(x,y,z) = v_0(z) + x\Theta(z), \quad (2)$$

$$w(n,s,z) = w_0(z) + x(s)\theta_y(z) + y(s)\theta_x(z) - F_\omega(s)\Theta'(z) + n \left[\frac{dy}{ds} \theta_y(z) - \frac{dx}{ds} \theta_x(z) - a(s)\Theta'(z) \right], \quad (3)$$

where

$$\theta_y(z) = \gamma_{xz}(z) - u_0'(z), \quad (4)$$

$$\theta_x(z) = \gamma_{yz}(z) - v_0'(z), \quad (5)$$

$$a(s) = -y(s) \frac{dy}{ds} - x(s) \frac{dx}{ds}. \quad (6)$$

The warping function is expressed as

$$F_\omega(s) = \int_0^s [r_n(s) - \psi] ds, \quad (7)$$

where the torsional function ψ is given by

$$\psi = \frac{\oint_C r_n(s) \frac{ds}{h(s)}}{\oint_C \frac{ds}{h(s)}} \left[\equiv \frac{2A_C}{\beta} \right], \quad (8)$$

and

$$r_n(s) = x(s) \frac{dy}{ds} - y(s) \frac{dx}{ds}. \quad (9)$$

As a result, six kinematic variables $u_0(z)$, $v_0(z)$, $w_0(z)$, $\theta_y(z)$, $\theta_x(z)$, and $\Theta(z)$ representing three translations in the x , y , z directions and three rotations about the y , x , and z axis, respectively, are used to define the displacement vector (i.e., the displacement components u , v , and w in the x , y , and z directions, respectively). Here (s, z, n) and (x, y, z) will be used to denote the surface and cross-section reference coordinate systems, respectively (see F1). The quantity $h[\equiv h(s)]$ denotes the wall thickness of the beam (allowed to vary along the periphery); A_C denotes the

cross-sectional area bounded by the mid-line; β denotes the total length of the contour mid-line; $\oint_C (\cdot) ds$ denotes the integral around the entire periphery C of the mid-line cross-section of the

beam; while $\int_0^s r_n(s) ds [\equiv \Omega(s)]$ is referred to as the sectorial area.

Based on the kinematic representations, Eqs. (1)–(6), the strain measures assume the form:

Axial Strain:

$$S_{zz}(n, s, z) = \bar{S}_{zz}(s, z) + n \bar{\bar{S}}_{zz}(s, z), \quad (10)$$

where

$$\bar{S}_{zz}(s, z) = w'_0(z) + \theta'_y(z)x(s) + \theta'_x(z)y(s) - \Theta''(z)F_\omega(s), \quad (11)$$

and

$$\bar{\bar{S}}_{zz}(s, z) = \theta'_y(z) \frac{dy}{ds} - \theta'_x(z) \frac{dx}{ds} - \Theta''(z)a(s),$$

are the axial strains associated with the primary and secondary warping, respectively.

Membrane Shear Strain:

$$S_{sz}(s, z) = [\theta_y(z) + u'_0(z)] \frac{dx}{ds} + [\theta_x(z) + v'_0(z)] \frac{dy}{ds} + 2 \frac{A_C}{\beta} \Theta'(z). \quad (12)$$

Transverse Shear Strain:

$$S_{nz}(s, z) = [\theta_y(z) + u'_0(z)] \frac{dy}{ds} - [\theta_x(z) + v'_0(z)] \frac{dx}{ds}. \quad (13)$$

Within the present theory the warping measure is expressible as

$$W_M = \Theta'(z). \quad (14)$$

Here, and in the following developments $(\cdot)' \equiv \partial(\cdot)/\partial z$.

PIEZOELECTRIC CONSTITUTIVE EQUATIONS

The linear constitutive equations for a 3-D piezoelectric continuum expressed in the contracted indicial notations are (see e.g., R13,14):

$$\begin{aligned} \sigma_i &= C_{ij}^{\mathcal{S}} S_j - e_{ki} \mathcal{E}_k, \\ D_k &= e_{kj} S_j + \epsilon_{kl}^{\mathcal{S}} \mathcal{E}_l, \end{aligned} \quad (15)$$

where σ_i and S_j ($i, j = \overline{1,6}$) denote the stress and strain components, respectively, where

$$S_j = \begin{cases} S_{pr} & \text{when } p = r, j = 1, 2, 3 \\ 2S_{pr} & \text{when } p \neq r, j = 4, 5, 6 \end{cases}$$

$C_{ij}^{\mathcal{S}}$, e_{ki} , $\epsilon_{kl}^{\mathcal{S}}$ are the elastic (measured for conditions of constant electric field), piezoelectric, and dielectric constants (measured under constant strain), while \mathcal{E}_k and D_k ($k = \overline{1,3}$) denote the electric field intensity and electric displacement vector, respectively. In Eqs. (15) the summation over repeated indices is implied. While Eq. (15)₁ describes the converse piezoelectric effect (consisting of the generation of mechanical stress or strain when an electric field is applied), Eq. (15)₂ describes the direct piezoelectric effect (consisting of generation of an electrical charge when a mechanical force or pressure is applied).

In a piezoelectric adaptive structure the direct effect is used for distributed sensing while the converse effect is used for the active distributed control. Equations (15) are valid for the most general anisotropic case, i.e., for triclinic crystals. In the following, we will restrict the generality to the case of a transversely isotropic continuum, the n -axis being an axis of rotary symmetry coinciding with the direction of polarization (thickness polarization).

In this case the piezoelectric continuum is characterized by 5 independent elastic constants, 3 independent piezoelectric constants and 2 independent dielectric constants. In the following developments, for the sake of simplicity, we will assume that the master structure is constructed from transversely isotropic material layers, the axis of symmetry being parallel to the n -axis.

We will also assume that the electric field vector \mathcal{E}_l is represented in terms of its component \mathcal{E}_3 only, (implying $\mathcal{E}_1 = \mathcal{E}_2 = 0$) and, as a result of the uniform voltage distribution, \mathcal{E}_3 is independent of space (but, possibly on time). In matrix form the constitutive equations are:

$$\begin{bmatrix} \sigma_1 \\ \sigma_2 \\ \sigma_3 \\ \sigma_4 \\ \sigma_5 \\ \sigma_6 \end{bmatrix}_{(k)} = \begin{bmatrix} C_{11} & C_{12} & C_{13} & & & \\ C_{12} & C_{11} & C_{13} & & & \\ C_{13} & C_{13} & C_{33} & & & \\ & & & C_{44} & & \\ & & & & C_{44} & \\ & & & & & \frac{C_{11}-C_{12}}{2} \end{bmatrix}_{(k)} \begin{bmatrix} S_1 \\ S_2 \\ S_3 \\ S_4 \\ S_5 \\ S_6 \end{bmatrix}_{(k)}$$

$$- \begin{bmatrix} 0 & 0 & e_{31} \\ 0 & 0 & e_{31} \\ 0 & 0 & e_{33} \\ 0 & e_{15} & 0 \\ e_{15} & 0 & 0 \\ 0 & 0 & 0 \end{bmatrix}_{(k)} \begin{bmatrix} 0 \\ 0 \\ \alpha_3 \end{bmatrix}_{(k)} \quad (16)$$

and

$$\begin{bmatrix} D_1 \\ D_2 \\ D_3 \end{bmatrix}_{(k)} = \begin{bmatrix} 0 & 0 & 0 & 0 & e_{15} & 0 \\ 0 & 0 & 0 & e_{15} & 0 & 0 \\ e_{31} & e_{31} & e_{33} & 0 & 0 & 0 \end{bmatrix}_{(k)} \begin{bmatrix} S_1 \\ S_2 \\ S_3 \\ S_4 \\ S_5 \\ S_6 \end{bmatrix}_{(k)} \quad (17)$$

$$+ \begin{bmatrix} \epsilon_{11} & 0 & 0 \\ 0 & \epsilon_{11} & 0 \\ 0 & 0 & \epsilon_{33} \end{bmatrix}_{(k)} \begin{bmatrix} 0 \\ 0 \\ \alpha_3 \end{bmatrix}_{(k)}$$

where the index k in brackets affecting a quantity identifies its affiliation to the k -th layer. In terms of the engineering constants the coefficients C_{ij} associated with a transversely-isotropic continuum are expressed as (where for the sake of simplification the

superscript δ was discarded):

$$\begin{aligned}
 C_{11} &= (E\nu'^2 - E')E/\Delta, \\
 C_{12} &= -(E\nu'^2 + E'\nu)E/\Delta, \\
 C_{13} &= -\nu'(1+\nu)EE'/\Delta, \\
 C_{33} &= -(1-\nu'^2)E'^2/\Delta, \quad C_{44} = G', \\
 \frac{C_{11}-C_{12}}{2} &= G(\equiv \frac{E}{2(1+\nu)}),
 \end{aligned} \tag{18}$$

where $\Delta = (1+\nu)(2E\nu'^2 + E'\nu - E')$ while E , ν , and E' , ν' denote Young's modulus and Poisson's ratio in the plane of isotropy and transverse to the plane of isotropy, respectively while G' denotes the transverse shear modulus. Equation (16) reveals that a piezoelectric continuum exhibiting anisotropic behavior cannot generate or detect shear stresses/strains by applying or detecting electric fields along the n -direction.

INCORPORATION OF ACTUATOR PATCHES AND ASSOCIATED CONSTITUTIVE EQUATIONS

As was stated earlier, the master structure is composed of layers of elastic materials also exhibiting transversely-isotropic behavior. Their associated constitutive equations could be established formally by discarding the electrical effects in Eq. (16) and Eq. (17).

Suppose that the master structure is composed of such layers, while the actuator (superposed on the master structure) is composed of ℓ piezoelectric layers. We also stipulate that the actuators are distributed over the entire span of the wing (i.e., along the entire spanwise coordinate z), (see F2) while along the circumferential s - and transversal n -directions they are distributed according to the law (see F3):

$$\begin{aligned}
 R_{(k)}(n) &= H(n - n_{(k^-)}) - H(n - n_{(k^+)}) , \\
 R_{(k)}(s) &= H(s - s_{(k^-)}) - H(s - s_{(k^+)}) ,
 \end{aligned} \tag{19}$$

where H denotes Heaviside's distribution and R is a spatial function [R15]. In terms of the coordinates (s, z, n) , related to the beam, the constitutive equations are expressed as

$$\begin{bmatrix} \sigma_{ss} \\ \sigma_{zz} \\ \sigma_{sz} \end{bmatrix}_{(k)} = \begin{bmatrix} C_{11} & C_{12} & 0 \\ C_{12} & C_{11} & 0 \\ 0 & 0 & \frac{C_{11}-C_{12}}{2} \end{bmatrix}_{(k)} \begin{bmatrix} S_{ss} \\ S_{zz} \\ S_{sz} \end{bmatrix}_{(k)} - \begin{bmatrix} e_{31}^{(k)} \delta_3^{(k)} R_{(k)(n)} R_{(k)(s)} \\ e_{31}^{(k)} \delta_3^{(k)} R_{(k)(n)} R_{(k)(s)} \\ 0 \end{bmatrix}$$

and

$$\sigma_{nz}^{(k)} = C_{44}^{(k)} S_{nz}^{(k)} \quad (20)$$

LOCAL BEAM CONSTITUTIVE RELATIONSHIPS

Assume that the master structure is composed of m layers while the actuator part is composed of ℓ layers. As a result, the global beam stress resultants and couples could be obtained through the integration of the 3-D stress components through the laminate thickness and afterwards through the integration of the local stress resultants along the contour of the beam. Invoking the assumption 5), the local beam stress resultants defined in terms of the associated strains are:

Stress Resultants:

$$N_{zz} = \bar{K}_{11} \bar{S}_{zz} + \bar{K}_{11} \bar{S}_{zz} - N_{zz}^a,$$

$$N_{sz} = A_{66} S_{sz},$$

$$N_{nz} = A_{44} S_{nz},$$

(21)

Stress Couples:

$$L_{zz} = \bar{K}_{11} \bar{S}_{zz} + \bar{K}_{11} \bar{S}_{zz} - L_{zz}^a,$$

$$L_{sz} = B_{66} S_{sz}.$$

In these equations K_{ij} denote the modified local stiffness coefficients while N_{zz}^a and L_{zz}^a the piezoelectrically induced stress resultant and stress couple. Their expressions are

$$\bar{K}_{11} = A_{11} - \frac{A_{12}^2}{A_{11}}; \quad \bar{K}_{11} = B_{11} - \frac{B_{12} A_{12}}{A_{11}},$$

$$\bar{K}_{11} = D_{11} - \frac{B_{12}^2}{A_{11}} \quad (22)$$

$$N_{zz}^a = \left[1 - \frac{A_{12}}{A_{11}}\right] \sum_{k=1}^{\ell} \alpha_3^{(k)} \left[n_{(k^+)} - n_{(k^-)} \right] e_{31}^{(k)} R_{(k)}(s, z) \quad (23)$$

$$L_{zz}^a = \sum_{k=1}^{\ell} \alpha_3^{(k)} e_{31}^{(k)} R_{(k)}(s, z) \left[n_{(k^+)} - n_{(k^-)} \right] \left[\frac{1}{2} \left[n_{(k^+)} + n_{(k^-)} \right] - \frac{B_{12}}{A_{11}} \right]$$

whereas

$$A_{ij} = \sum_{k=1}^{m+\ell} C_{ij}^{(k)} \left[n_{(k)} - n_{(k-1)} \right]$$

$$B_{ij} = \frac{1}{2} \sum_{k=1}^{m+\ell} C_{ij}^{(k)} \left[n_{(k)}^2 - n_{(k-1)}^2 \right] \quad (24)$$

$$D_{ij} = \frac{1}{3} \sum_{k=1}^{m+\ell} C_{ij}^{(k)} \left[n_{(k)}^3 - n_{(k-1)}^3 \right]$$

define the stretching, bending-stretching and bending stiffness quantities, respectively. In Eqs. (23), for the sake of brevity the following notation

$$R_{(k)}(s, z) \equiv R_{(k)}(s)R_{(k)}(z) \quad (25)$$

was introduced.

It should be emphasized that the constitutive equations (21) relate the stress resultants and couples with the strain components and the electric field, α_3 . The analysis yielding such equations is called uncoupled because an approximate solution to the electrostatic problem is postulated, with the result that α_3 is constant.

THE DYNAMIC EQUATIONS OF ADAPTIVE THIN-WALLED BEAMS

In the previous sections the kinematic equations and the local constitutive equations for the considered adaptive structure were derived. In order to obtain the equation of motion of an adaptive TWB and the associated boundary conditions, we will make use of Hamilton's variational principle extended to the case of a linear 3-D piezoelectric medium [R5,6]:

$$\delta \int_{t_0}^{t_1} dt \left[\int_{\tau} \left[\frac{1}{2} \rho \dot{U}_i \dot{U}_i - \mathcal{H} + f_i U_i \right] d\tau + \int_{\Omega} (\bar{\sigma}_k \delta U_k - \bar{\sigma} \delta \phi) d\Omega \right] = 0, \quad (26)$$

where \mathcal{H} denotes the electric enthalpy density defined as:

$$\mathcal{H} = \frac{1}{2} C_{ij}^E S_i S_j - e_{ki} \xi_k S_i - \frac{1}{2} \epsilon_{kl}^S \xi_k \xi_l, \quad (27)$$

τ and Ω denote the volume and bounding surface of the continuum, respectively; $\bar{\sigma}_k$ denotes the specified surface-traction; $\bar{\sigma}$ the applied surface charge; f_i the body forces; t_0, t_1 denote two arbitrary instants of time; ρ the material density; δ the variation sign, while the overdots denote time derivatives.

Recalling that

$$\frac{\partial \mathcal{H}}{\partial S_i} = \sigma_i \quad \text{and} \quad \frac{\partial \mathcal{H}}{\partial \xi_k} = -D_k, \quad (28)$$

when $\delta \xi_i = 0$, defining ξ_i in terms of a potential function as

$$\xi_i = -\phi_{,i}, \quad (29)$$

taking the variations in (26) and applying Green's theorem whenever possible, we obtain, by considering the variations δU_i , $\delta \phi$ and $\delta \sigma_i$ as independent and arbitrary, a known version of the fundamental equations of the 3-D linear piezoelectricity theory, namely

$$\left. \begin{aligned} \sigma_{ij,j} + f_i &= \rho \ddot{U}_i \\ D_{i,i} &= 0 \end{aligned} \right\} \text{in } \tau, \quad (30)$$

$$\bar{\sigma}_i = \sigma_{ij} n_j \quad \phi = \bar{\phi} \text{ on } \Omega_s,$$

$$U_i = \bar{U}_i \quad \bar{\sigma} = n_i D_i \text{ on } \Omega_u,$$

are obtained, where n_i denote the components of the normal to Ω . Consideration in Eq. (26) of the displacement components U_i as $u_0, v_0, w_0, \theta_x, \theta_y$, and Θ , and of S_i as the ones defined by Eqs. (10)–(13); employment of $d\tau = dn ds dz$ and performing the integration across the s - and n -directions, the 3-D problem is reduced to an equivalent 1-D one, in which all the quantities are dependent on the z -coordinate only. To this end, the 1-D stress resultants and stress couples specific to the theory of TWBs defined in terms of the local (i.e., 2-D) beam stress-resultants are

$$\begin{aligned} T_z(z) &\equiv \oint_C N_{zz} ds; \quad Q_x(z) = \oint_C \left[N_{sz} \frac{dx}{ds} + N_{zn} \frac{dy}{ds} \right] ds, \\ Q_y(z) &= \oint_C \left[N_{sz} \frac{dy}{ds} - N_{zn} \frac{dx}{ds} \right] ds, \quad M_x(z) = \oint_C \left[y N_{zz} - L_{zz} \frac{dx}{ds} \right] ds, \end{aligned} \quad (31)$$

$$M_y(z) = \oint_C \left[xN_{zz} + L_{zz} \frac{dy}{ds} \right] ds ; M_z(z) = \oint_C N_{sz} \frac{2A_C}{\beta} ds ,$$

and

$$B_\omega(z) = \oint_C [F_\omega(s)N_{zz} + a(s)L_{zz}] ds .$$

These quantities are referred to as the axial and shear forces (in the x and y directions), and the moments (in the x, y and z directions) as well as the bimoment global quantities. In terms of the 1-D stress resultant measures, (Eq. 31), the equations of motion of adaptive TWBs become:

$$\begin{aligned} \delta u_0: \quad Q'_x - I_1 + p_x &= 0 , \\ \delta v_0: \quad Q'_y - I_2 + p_y &= 0 , \\ \delta w_0: \quad T'_z - I_3 + p_z &= 0 , \\ \delta \Theta: \quad B'_\omega + M'_z - (I_4 - I_8') + m_z + b'_\omega &= 0 , \\ \delta \theta_x: \quad M'_x - Q_y - I_5 + m_x &= 0 , \\ \delta \theta_y: \quad M'_y - Q_x - I_7 + m_y &= 0 . \end{aligned} \tag{32}$$

Here p_x , p_y , p_z and m_x , m_y and m_z are the distributed loads and moments in the x, y, and z-directions, respectively; b_ω is the bimoment of the external loads while I_i ($i = \overline{1,8}$) are the inertia terms not displayed in the paper. By virtue of Eqs. (21), (23) and (31) the stress resultant T_z , the stress couples M_x and M_y as well as the bimoment B_ω could be recast in a form in which the actuator effect appears in a separated form, namely

$$\begin{aligned} T_z &= \hat{T}_z - \tilde{T}_z ; \quad M_x = \hat{M}_x - \tilde{M}_x , \\ M_y &= \hat{M}_y - \tilde{M}_y ; \quad B_\omega = \hat{B}_\omega - \tilde{B}_\omega , \end{aligned} \tag{33}$$

where the quantities affected by an overhat ($\hat{\quad}$) and an overtilde ($\tilde{\quad}$) identify the pure mechanical and piezoelectric contributions to the indicated quantities, respectively.

Being concerned in this study with the free vibration problem only, the loading terms occurring in Eqs. (32) may be discarded. From the Hamilton's principle, in addition to the equations of motion (32), the boundary conditions (BCs) are also obtained. For the case of the beam clamped at $z = 0$ and free at $z = L$, the BCs are:

At the clamping edge ($z = 0$):

$$\underline{u}_0 = \underline{u}_0; \underline{v}_0 = \underline{v}_0; \underline{w}_0 = \underline{w}_0; \underline{\theta}_x = \underline{\theta}_x; \underline{\theta}_y = \underline{\theta}_y; \underline{\Theta} = \underline{\Theta}; \underline{\Theta}' = \underline{\Theta}' \quad (34)$$

and at the free edge ($z = L$):

$$\underline{Q}_x = \underline{Q}_x; \underline{Q}_y = \underline{Q}_y; \underline{T}_z = \underline{T}_z; \underline{M}_y = \underline{M}_y; \underline{M}_x = \underline{M}_x, \\ \underline{M}_z + \underline{B}'_\omega = \underline{M}_z; \underline{B}_\omega = \underline{B}_\omega, \quad (35)$$

where the undertilde sign affects the prescribed quantities and where L denotes the length of the beam. It could be verified that consistent with seven boundary conditions at each edge, a fourteenth order governing equation system is obtained.

In the case of the general anisotropy of the layer materials (i.e., of the master structure, of the actuator patches or of both of them), the system of governing equations results in a complete coupled form. However, in the present case of anisotropy, the governing equations obtainable from Eqs. (32)_{1,6} appear decoupled from the ones obtainable from (32)_{2,5} and (32)_{3,4}. In other words, in the present case of anisotropy, the governing system of equations and the associated BCs are splitting exactly into three uncoupled sub-systems. While the first mentioned sub-system of equations governs the lateral bending motion (or in helicopter terminology, the flap-lag motion), the second and the third ones govern the vertical bending and twist motions, respectively.

In this study only the undamped free bending vibration case is studied. The pertinent governing equations for free vibration of thin-walled beams are:

For transverse bending vibrations:

$$a_{55}(\underline{v}_0'' + \underline{\theta}_x') + b_1 \omega^2 \underline{v}_0 = 0 \\ a_{33} \underline{\theta}_x'' - a_{55}(\underline{v}_0' + \underline{\theta}_x) + \omega^2(b_4 + b_{14}) \underline{\theta}_x = 0. \quad (36)$$

with the BCs at $z = 0$:

$$\underline{v}_0 = \underline{\theta}_x = 0 \quad (37)$$

and at $z = L$:

$$\underline{v}_0' + \underline{\theta}_x = 0 \quad \text{and} \quad a_{33} \underline{\theta}_x' = \underline{\tilde{M}}_x \quad (38)$$

For lateral bending vibrations:

$$a_{44}(\underline{u}_0'' + \underline{\theta}_y') + b_1 \omega^2 \underline{u}_0 = 0 \quad (39)$$

$$a_{22}\theta_y'' - a_{44}(u_0' + \theta_y) + \omega^2(b_5 + b_{15})\theta_y = 0$$

with the BCs at $z = 0$:

$$u_0 = \theta_y = 0 \quad (40)$$

and at $z = L$:

$$u_0' + \theta_y = 0 \quad \text{and} \quad a_{22}\theta_y' = \tilde{M}_y \quad (41)$$

These equations were obtained by considering the following harmonic time-dependence

$$\mathcal{F}(z,t) = \bar{\mathcal{F}}(z)\exp(i\omega t), \quad i = \sqrt{-1} \quad (42)$$

where \mathcal{F} stands for a generic field variable.

Both the governing equations and the associated BCs are expressed in terms of the quantities involving the dependence on the s -coordinate only, i.e., according to Eq. (42) in terms of the barred counterparts of the field variables. However, for the sake of simplicity these overbars have been dropped. The expressions of elastic constants a_{ij} and mass terms b_i

intervening in Eqs. (36) and (39) are not displayed here. In the same equations \tilde{M}_x and \tilde{M}_y denote the piezoelectrically induced moments expressed as:

$$\begin{aligned} \tilde{M}_x = & \int_C \sum_{k=1}^{\ell} a_3^{(k)} \left[n_{(k^+)} - n_{(k^-)} \right] e_{31}^{(k)} R_{(k)}(s,z) \left[y \left[1 - \frac{A_{12}}{A_{11}} \right] \right. \\ & \left. + \frac{dx}{ds} \frac{B_{12}}{A_{11}} \right] ds - \frac{1}{2} \int_C \left[\frac{dx}{ds} \sum_{k=1}^{\ell} a_3^{(k)} \left[n_{(k^+)}^2 - n_{(k^-)}^2 \right] e_{31}^{(k)} R_{(k)}(s,z) \right] ds, \\ \tilde{M}_y = & \int_C \sum_{k=1}^{\ell} a_3^{(k)} \left[n_{(k^+)} - n_{(k^-)} \right] e_{31}^{(k)} R_{(k)}(s,z) \left[x \left[1 - \frac{A_{12}}{A_{11}} \right] \frac{dy}{ds} \frac{B_{12}}{A_{11}} \right] ds \\ & + \frac{1}{2} \int_C \left[\frac{dy}{ds} \sum_{k=1}^{\ell} a_3^{(k)} \left[n_{(k^+)}^2 - n_{(k^-)}^2 \right] e_{31}^{(k)} R_{(k)}(s,t) \right] ds \end{aligned} \quad (43)$$

For the case of the symmetrically located actuators across the thickness of the beam structure, the terms affected by a solid line in Eqs. (43) vanish. In light of the actuator configuration, it may be inferred that the expressions (43) are independent on the z -coordinate. This explains why their contribution in the governing equations is immaterial and why in the BCs they intervene as nonhomogeneous terms.

THE CONTROL LAW

The adaptive nature of the wing (or rotor blade) structure is introduced by requiring the applied electric field \mathcal{E}_j to be dependent to one of the mechanical quantities of the structure in motion. With this in mind, a number of control laws could be implemented. Their efficiency may be measured by their ability to modify as much as possible the natural frequencies of the structure with respect to the energy input. In the present considerations, two control laws were considered.

The two independent control laws require that: i) the applied electric field \mathcal{E}_j is proportional to the vertical or lateral bending moments at the wing root, $\hat{M}_x(o)$ or $\hat{M}_y(o)$, depending on whether the control of the natural frequencies is associated with the vertical or lateral motion, respectively and ii) the applied electric field \mathcal{E}_j is proportional to the vertical ($v_o(L)$) or lateral ($u_o(L)$) deflections of the beam tip, depending on the two directions of vibrations whose frequencies are to be controlled. In light of these control approaches, we may formulate the following control laws (labelled as CL1 and CL2) by involving also the boundary conditions given in expression (38) and (41).

CL1)

a) Associated with the vertical bending

$$\theta_x'(L) = K_p \theta_x'(o) \quad (44)$$

b) Associated with the lateral bending

$$\theta_y'(L) = K_p \theta_y'(o) \quad (45)$$

CL2)

a) Associated with the vertical bending

$$\theta_x'(L) = \bar{K}_p v_o(L) \quad (46)$$

b) Associated with the lateral bending

$$\theta_y'(L) = \bar{K}_p u_o(L) \quad (47)$$

As can be seen from Eqs. (44)–(47), the feedback gains \bar{K}_p and K_p are dimensional and nondimensional, respectively. The nondimensional counterpart of \bar{K}_p is \check{K}_p defined as $\check{K}_p = \bar{K}_p L^2$.

These control laws express the fact that the control bending moments at the wing tip (induced by the piezoelectric strain) should be proportional as per the CL1 to the mechanical bending moments at the wing root, and within the CL2 to the transversal or lateral deflections at the wing tip.

NUMERICAL ILLUSTRATIONS AND DISCUSSION

The adaptive wing is modelled as a symmetric composite box-beam. In order to control the vertical bending frequencies, the piezoceramic actuator layers (selected to be of PZT-4 ceramic) are located on the upper and bottom surfaces of the master structure only, while in order to control the lateral bending frequencies the piezoceramic layers are located on the lateral walls of the master structure. The geometrical characteristics (restricted to the former situation, only) are displayed in F2 while the constants characterizing the PZT-4 piezoceramic (see [R16]) are:

$$C_{11} = 2.016 \times 10^7 \text{ psi}; \quad C_{12} = 1.128 \times 10^7 \text{ psi}$$

$$C_{13} = 1.0776 \times 10^7 \text{ psi}; \quad C_{33} = 1.6679 \times 10^7 \text{ psi}$$

$$C_{44} = 3.7128 \times 10^6 \text{ psi};$$

$$e_{31} = -0.0297 \text{ lb/inV}; \quad e_{33} = 0.08623 \text{ lb/inV}$$

$$e_{15} = 0.07252 \text{ lb/inV}.$$

For the sake of simplicity assume that the master structure is composed of a transversely-isotropic material whose elastic characteristics are identical to the piezoceramic actuator layers.

By using the exact approach devised in [R17-19] and extended afterwards in [R7-9], the eigenvalue problems associated with the vertical and lateral vibrations of TWBs yield the variation of the nondimensional eigenfrequencies $\tilde{\omega}$ vs. the feedback gains K_p and \check{K}_p .

In F4-7, by using the control law CL1, the variation of the first four eigenfrequencies associated with the vertical bending vs. the feedback gain was diagrammatically represented, while in F8 and 9, by using the control law CL2, the variation of the vertical (plunging) and lateral bending fundamental frequencies $\tilde{\omega}$ vs. the feedback gain \check{K}_p was obtained. F4-7 reveal that within control law CL1 the increase of the odd eigenfrequencies occurs for negative feedback gains while the increase of the even eigenfrequencies requires implementation of positive feedback gains. F8 and 9 (as well as the results obtained, but not displayed in the paper) reveal that within control law CL2 the increase of the eigenfrequencies occurs generally for positive feedback gains. Within a CL2 type control a similar trend was also obtained in R20.

It should be pointed out that in all diagrams, F4-9, the frequencies were normalized with respect to the ones corresponding to the non-adaptive structure (for which case $K_p = 0$).

Having in view that, roughly speaking, $\omega \sim D^{1/2} \sim h^{3/2}$, where D and h are the associated bending rigidity and thickness of the beam, we could infer that the linear increase of eigenfrequencies would have been accomplished without the help of this adaptive technology through an unaffordable weight penalty. The obtained results reveal, once again, the great importance of the implementation of adaptive technology applied to the control of the material frequencies of the structure. In short, the obtained results reveal that by using the adaptive properties of the structure it is possible to increase the eigenfrequencies of the system and consequently to modify in a beneficial way the dynamic response characteristics of the structure, whose role in the present case could be played by an aircraft wing or a rotor blade structure.

ACKNOWLEDGEMENT

The partial support of this work by the Office of Naval Research (ONR/DARPA Grant N00014-88-0721) is gratefully acknowledged.

REFERENCES

1. Rogers, C. A., "An Introduction to Intelligent Material Systems and Structures," in Intelligent Structures, pp. 3-41, (Eds. Chong, K. P., Liu, S. C. and Li, J. C.), Elsevier Applied Science, London and New York, 1990.
2. Librescu, L., Elastostatics and Kinetics of Anisotropic and Heterogeneous Shell-Type Structures, Noordhoff International Publ., The Netherlands, 1975.
3. Wang, B.-T. and Rogers, C. A., "Laminate Plate Theory for Spatially Distributed Induced Strain Actuators," Journal of Composite Materials, Vol. 25, No. 4, April 1991, pp. 433-452.
4. Wang, B.-T. and Rogers, C. A., "Modeling of Finite-Length Spatially-Distributed Induced Strain Actuators for Laminate Beams and Plates," Journal of Intelligent Material Systems and Structures, Vol. 2, No. 1, January 1991, pp. 38-58.
5. Tiersten, H. F., Linear Piezoelectric Plate Vibrations, Plenum Press, New York, 1969.
6. Lee, P. C. Y. and Haynes, D. W., "Piezoelectric Crystals and Electro-Elasticity," R. D. Mindlin and Applied Mechanics, (Ed. G. Hermann), Pergamon Press, 1977, pp. 227-253.
7. Librescu, L. and Song, O., "Static Aeroelastic Tailoring of Composite Aircraft Swept Wings Modelled as Thin-Walled Beam Structures," in "Achievements in Composites in Japan and the United States," Ed. A. Kobayashi, Fifth Japan-U.S. Conference on Composite Materials, Tokyo, Japan, June 24-27, 1990, pp. 141-149.
8. Librescu, L. and Song, O., "Behavior of Thin-Walled Beams Made of Advanced Composite Materials and Incorporating Non-Classical Effects," in "Mechanics Pan-America", 1991, Applied Mechanics Review, Eds. R.A. Kitte and D.T. Mook, Vol. 44, No. 11, Part 2, Nov. 1991, pp. 174-180.
9. Song, O. and Librescu, L., "Free Vibration and Aeroelastic Divergence of Aircraft Wings Modelled as Composite Thin-Walled Beams," The 32nd SDM Conference, Paper AIAA 91-1187, 1991.

10. Rehfield, L. W., Atilgan, A. R. and Hodges, D. H., "Nonclassical Behavior of Thin-Walled Composite Beams," Journal of the American Helicopter Society, Vol. 35, No. 2, April, 1990, pp. 42-50.
11. Gjelsvik, A., The Theory of Thin-Walled Bars, John Wiley & Sons, New York, 1981.
12. Rehfield, L. W., "Design Analysis Methodology for Composite Rotor Blades," Proceedings of the Seventh DoD/NASA Conference on Fibrous Composites in Structural Design, AFWAL-TR-85-3094, June, 1985, pp. v(a)-1) - v(a)-15).
13. Mason, W. P., Crystal Physics of Interaction Processes, Academic Press, New York and London, 1966.
14. IEEE Standard on Piezoelectricity, IEEE Std. 176-1978, The Institute of Electrical and Electronics Engineers, Inc., 1978.
15. Wang, B.-T. and Rogers, C. A., "Laminate Plate Theory for Spatially Distributed Induced Strain Actuators," in "Achievements in Composites in Japan and the United States," A. Kobayashi, Ed., Fifth Japan-U.S. Conference on Composite Materials, Tokyo, Japan, June 24-27, 1990, pp. 595-607.
16. Berlincourt, D. A., Curran, D. R., and Jaffe, H., "Piezoelectric and Piezomagnetic Materials and Their Function in Transducers," Physical Acoustics - Principles and Methods, (Ed. W. P. Mason), Vol. 1, Part A, Academic Press, New York and London, 1964, pp. 169-270.
17. Librescu, L. and Thangjitham, S., "The Static Aeroelastic Behavior of Sweptforward Composite Wing Structures Taking Into Account Their Warping Restraint Effect," Proceedings of the Fourth Japan-U.S. Conference on Composite Materials, Washington, D.C., June 24-27, 1988, pp. 914-922.
18. Librescu, L. and Thangjitham, S., "The Warping Restraint Effect in the Critical and Subcritical Static Aeroelastic Behavior of Swept-Forward Composite Wing Structures," 1989 SAE General Aviation Aircraft Meeting and Exposition, Century II, Wichita, Kansas, April 11-13, 1989, Paper 891056.
19. Librescu, L. and Thangjitham, S., "Analytical Studies on Static Aeroelastic Behavior of Forward-Swept Composite Wing Structures," Journal of Aircraft, Vol. 28, 2, pp. 151-157, 1991.
20. Tzou, H.S. and Zhong, J.R., "Adaptive Piezoelectric Shell Structures: Theory and Experiments," AIAA Paper 91-1238-CP, 32nd AIAA SDM Conference, Baltimore, Maryland, April 8-12, 1991.

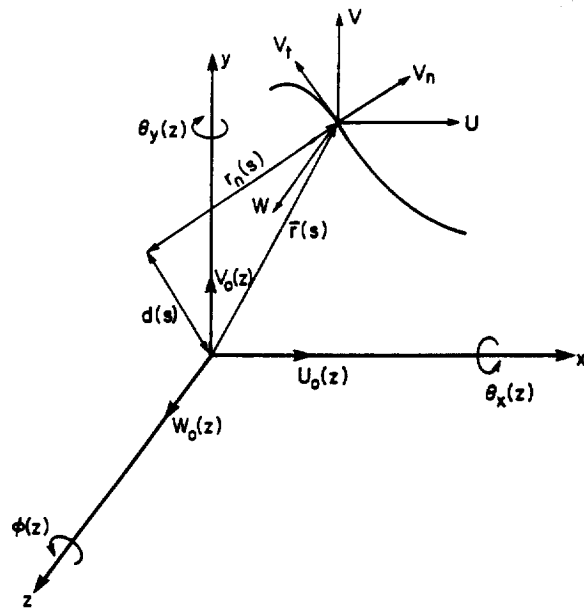


Fig. 1 Coordinate systems and Kinematic variables.

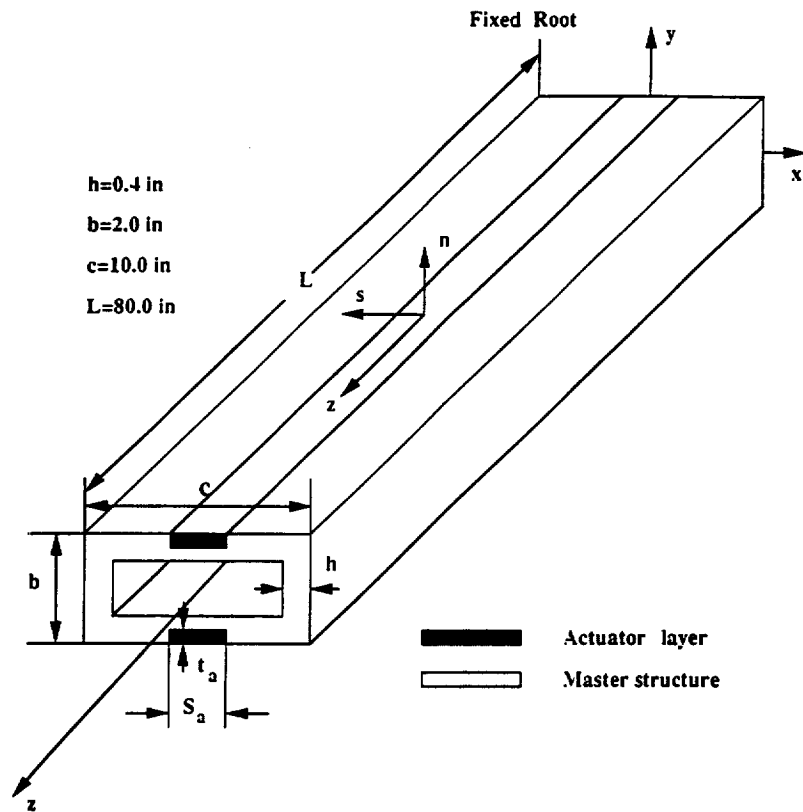


Fig. 2 Geometry of box beam (not scaled).

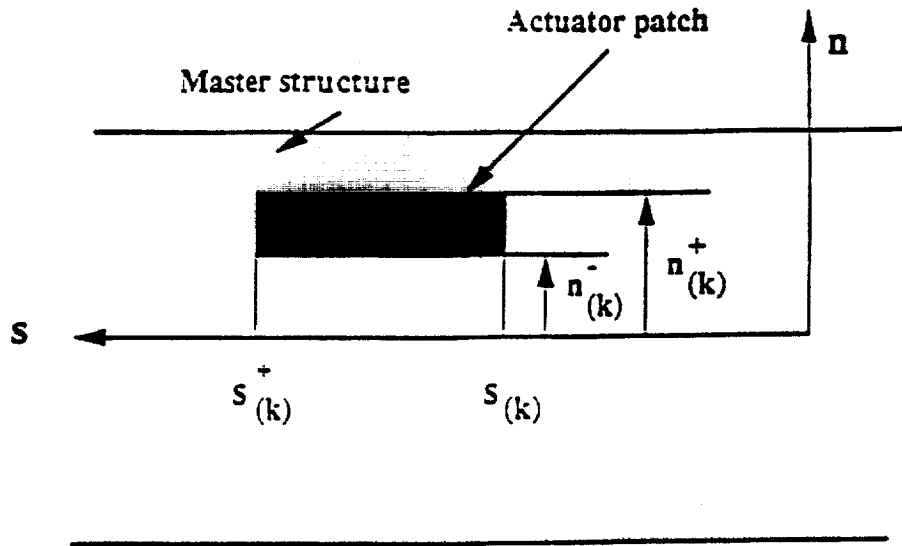


Fig. 3 Actuator patch.

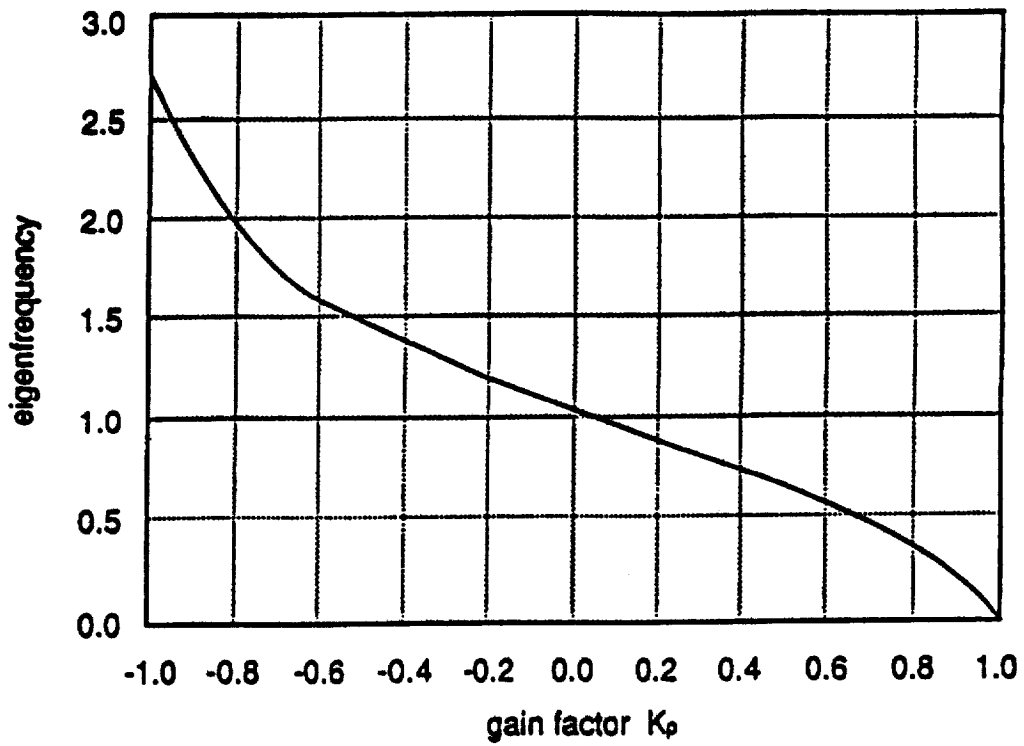


Fig. 4 Variation of the normalized plunging eigenfrequency vs. the control gain (first mode and first control law).

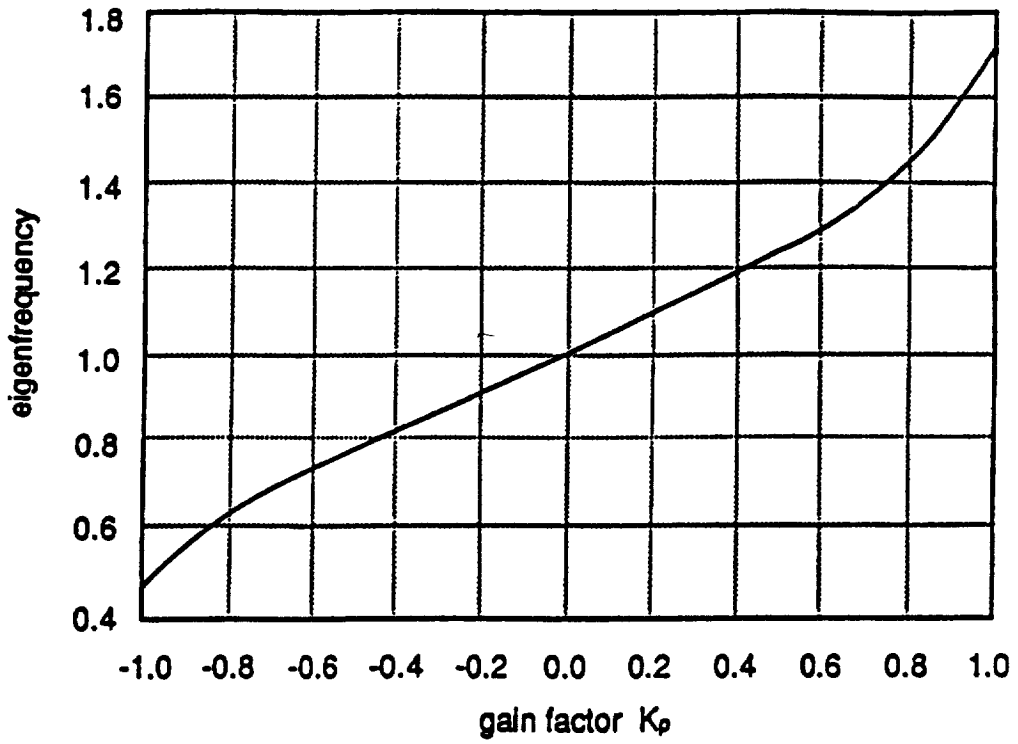


Fig. 5 Variation of the normalized plunging eigenfrequency vs. the control gain (second mode and first control law).

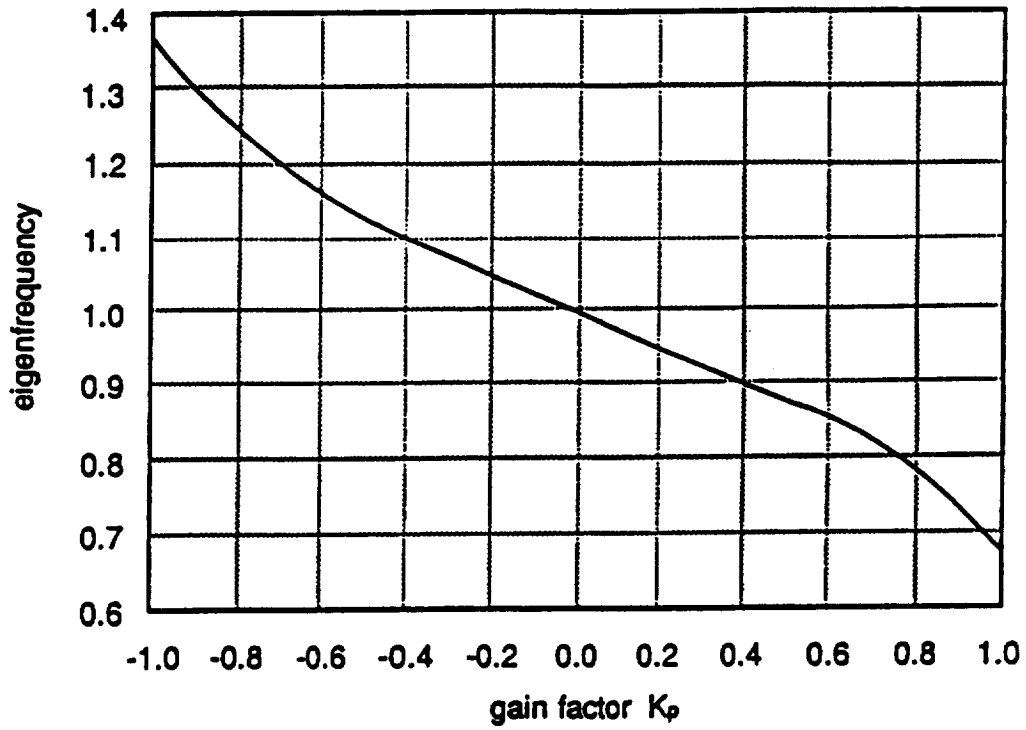


Fig. 6 Variation of the normalized plunging eigenfrequency vs. the control gain (third mode and first control law).

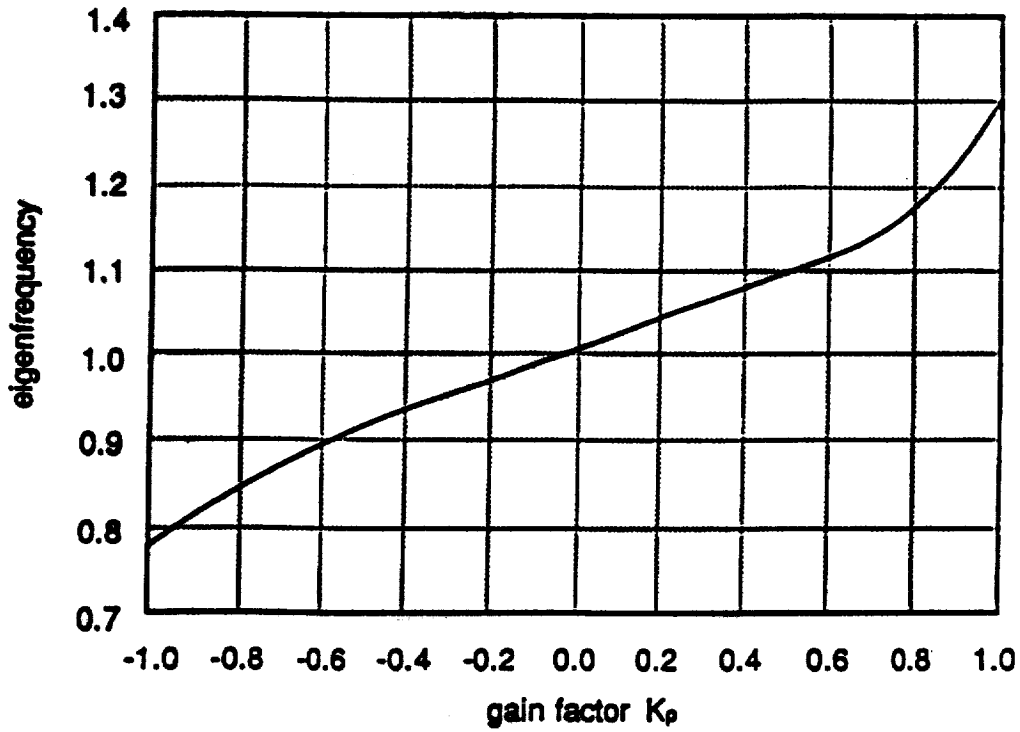


Fig. 7 Variation of the normalized plunging eigenfrequency vs. the control gain (fourth mode and first control law).

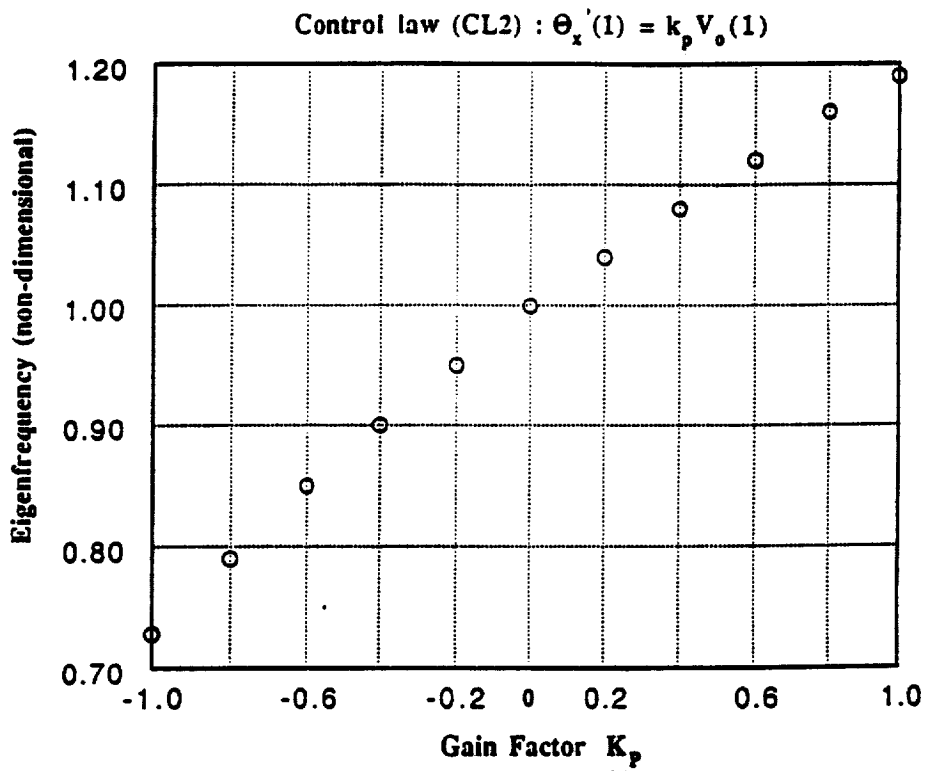


Fig. 8 Variation of the normalized plunging eigenfrequency vs. the control gain (first mode and second control law).

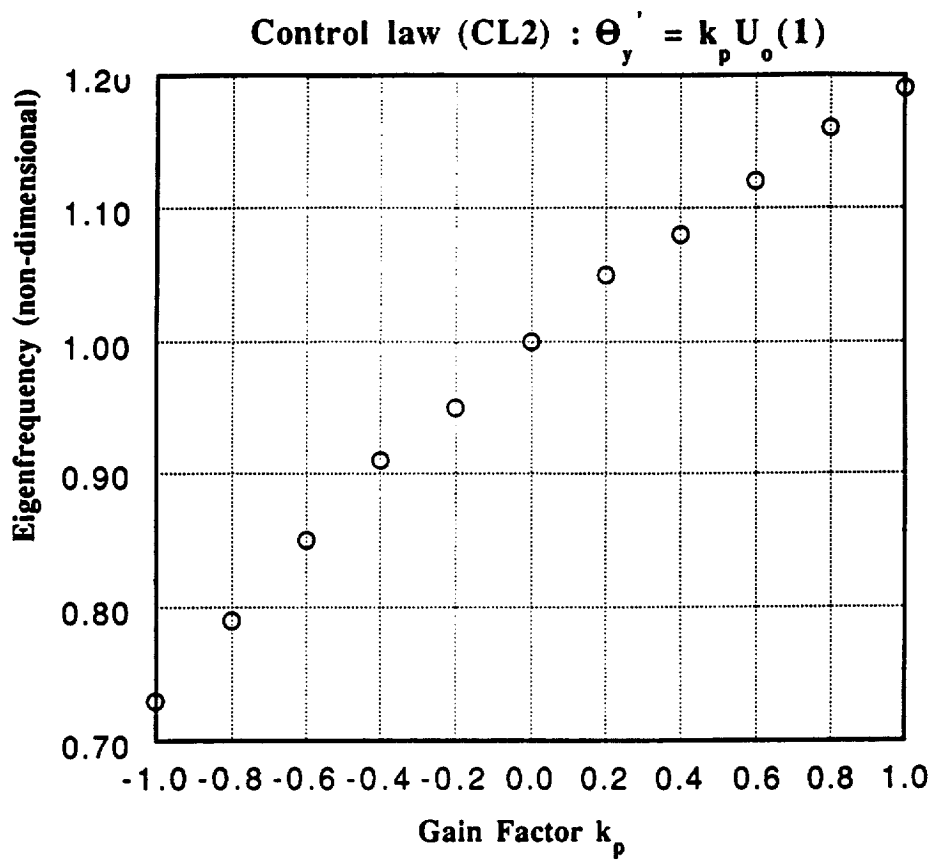


Fig. 9 Variation of the normalized lateral bending eigenfrequency vs. the control gain (first mode and second control law)

THIS PAGE INTENTIONALLY BLANK